



## Experimental study and mathematical modelling of convective thin-layer drying of noni (*Morinda citrifolia* L.)<sup>†</sup>

### Estudio experimental y modelado matemático del secado convectivo en capa fina de noni (*Morinda citrifolia* L.)

Francisco Canelo<sup>1\*</sup>, Kevin Gutiérrez<sup>1</sup>, Apolinar Picado<sup>2</sup>, Rafael Gamero<sup>1</sup>

<sup>1</sup>Facultad de Ingeniería Química, Universidad Nacional de Ingeniería (UNDI),  
Avenida Universitaria, Managua 11127, Nicaragua  
E-mail: [francisco.canelo@fiq.uni.edu.ni](mailto:francisco.canelo@fiq.uni.edu.ni)

<sup>2</sup>Department of Chemical Engineering, KTH Royal Institute of Technology  
Teknikringen 42, SE-100 Stockholm, Sweden

(recibido/received: 15-abril-2022; aceptado/accepted: 12-agosto-2022)

#### ABSTRACT

In this study, the drying kinetics of noni (*Morinda citrifolia* L.) was investigated in a laboratory tunnel dryer at air temperatures of 50, 60, and 70 °C and velocities of 1.0, 1.5, and 2.0 m/s. Noni showed only a falling drying rate period. Further, a non-linear regression procedure was used to determine the characteristic drying curve. The experimental drying data of noni were employed to fit thin-layer models. Under the evaluated experimental conditions, the Page model provided the best representation of thin-layer drying characteristics of noni. The effective moisture diffusivity ranged from  $1.77 \times 10^{-7}$  to  $3.33 \times 10^{-7}$  m<sup>2</sup>/s. The activation energy was found to be 3.34 kJ/mol.

**Keywords:** *Morinda citrifolia*; Mathematical modelling; Thin-layer drying; Regression analysis

#### RESUMEN

En este estudio, se investigó la cinética de secado del noni (*Morinda citrifolia* L.) en un secador de túnel de laboratorio a temperaturas de aire de 50, 60 y 70 °C y velocidades de 1.0, 1.5 y 2.0 m/s. Noni mostró solo un período de velocidad de secado decreciente. Además, se utilizó un procedimiento de regresión no lineal para determinar la curva de secado característica. Los datos experimentales de secado de noni se emplearon para ajustar modelos de capa fina. Bajo las condiciones experimentales evaluadas, el modelo de Page proporcionó la mejor representación de las características de secado de capa fina del noni. La difusividad de humedad efectiva osciló entre  $1.77 \times 10^{-7}$  y  $3.33 \times 10^{-7}$  m<sup>2</sup>/s. Se encontró que la energía de activación era de 3.34 kJ/mol.

**Palabra claves:** *Morinda citrifolia*; Modelado matemático; Secado en capa fina; Análisis de regresión

<sup>†</sup> In honour and loving memory of Prof. em. Dr.-Ing. habil. Luis Moreno (1942-2022).

---

\* Author for correspondence

## 1. INTRODUCTION

Noni (*Morinda citrifolia* L.) belongs to the *Rubiaceae* Juss. family and is a perennial plant, which is cultivated in many regions around the globe (e.g., Southeast Asia, Australia, Polynesia, India, the Caribbean, and the Americas). Noni fruit has shown various human health benefits, including antioxidant capacity, activity in bone regeneration, hypotensive activity, antibacterial activity, anti-inflammatory activity, activity against metabolic disorders associated with obesity (hyperlipidaemia and type 2 diabetes), and immune enhancement (Chan-Blanco *et al.*, 2006; Alonso and Guerrero-Santos, 2016; Wang *et al.*, 2022). It has thus attracted much attention from the food and pharmaceutical industries and general consumers.

Due to the potential therapeutic properties of the noni fruit, which distinguishes it from the best-known ones, it would be interesting to develop and characterise products from noni fruit to be used by the food industry as functional ingredients in the formulation of a vast range of health products and novel nutritional supplements. For instance, a variety of powders (from dried ripe or unripe fruits) and leaf powders (for encapsulation or pills) have been introduced into the consumer market (Nelson, 2003). In this context, the drying of fruits remains a very widespread operation in the food industry both for the preservation of fruits in their final form and as an intermediate operation.

Many fruits have been dried successfully including noni. Mireles-Arriaga *et al.* (2016) studied the effect of thin-layer drying temperature on colour, phenolic content, and antioxidant capacity of noni slices. Noni slices were air-dried at 50, 60 and 70 °C under natural convection conditions. Drying curves were fitted to thin-layer drying models to evaluate the drying characteristics of the product. Results revealed that the Aghbashlo model accurately reproduced the experimental behaviour. Effective moisture diffusivity was in the range from 1.80 to  $3.19 \times 10^{-9}$  m<sup>2</sup>/s. Recently, Lin *et al.* (2020) investigated the formation of aromatic esters in intermittently dried noni fruit by endogenous enzymatic activity. The whole ripe noni fruits were submitted to an intermittent drying process, which involved 8 h/day of mechanical drying at 50 °C and then tempered overnight in wooden boxes. The intermittent drying process was repeated for 14 days until reaching a moisture content of  $11 \pm 2$  % (wet basis). However, the conventional group was continuously dried at 50 °C until reaching a moisture content of  $11 \pm 2$  % (wet basis). The Newton model showed a good fit for the experimental data.

In addition, Quequeto *et al.* (2019) reported the drying of noni seeds under several controlled conditions of temperature, 40; 50; 60; 70 and 80 °C and relative humidity, 24.4; 16.0; 9.9; 5.7 and 3.3%, respectively. The seeds were dried on unperforated trays, which were periodically weighed with samples on a scale. The two-term model was selected to describe the drying kinetics of noni seeds. Effective moisture diffusivity ranged from 8.70 to  $23.71 \times 10^{-10}$  m<sup>2</sup>/s, and the activation energy was 24.20 kJ/mol for the studied temperature range.

Furthermore, Zhang *et al.* (2019) investigated the drying behaviour of fermented noni juice (FNJ) that includes different wall materials using the reaction engineering approach (REA). Single droplet drying was employed to study the basic parameters (diameter, mass, and temperature). The results illustrated that FNJ including M1 (maltodextrin, 10-13 DE) with 20 % solids content exhibited an earlier crust formation behaviour than that including M3 (maltodextrin, 17-20 DE) (28 %). The increased solids content of droplets caused a reduced shrinkage and an increased particle size.

To our knowledge, few studies have been published regarding the drying of noni fruit. The purpose of this study was to investigate the drying characteristics of noni fruit, as well as the suitability of several empirical and semi-empirical models available in the literature in defining the thin-layer drying characteristics of noni fruit. The effective diffusion coefficient at various temperatures and activation energy were estimated.

## 2. MATERIALS AND METHODS

### 2.1 Material

Noni fruits were procured from a local vegetable market, washed under running water to remove the impurities, and dried with a cloth. Noni fruits of similar size, shape, and free from injury were selected, unpeeled, and longitudinally sliced. The unpeeling step was necessary because the noni fruit's skin represents a barrier to moisture removal and higher exposure of the noni fruit improves water diffusion, thus shortening the drying process. Seeds were extracted before drying experiments.

### 2.2 Experimental apparatus

A schematic arrangement of the experimental apparatus is shown in Fig. 1. The equipment may be divided into four main sections as follows: gas supply and dehumidification section, heating section, drying chamber, and analysing equipment. The blower (B) supplies a gas flow—a broad range of flow rates is possible by changing the rpm setting through the frequency inverter (FI). The air passes through an adsorption column (AC) containing a dehumidificant (silica gel) to obtain a process air of low humidity content (less than 1.0 % relative humidity) measured by a hygrometer. The air velocity is measured by an anemometer. After dehumidification, the air is pre-heated with electrical resistance (ER) heaters of up to 2 kW each. Temperature is controlled by means of a temperature controller (TC) that supplies heat by means of an electrical resistance heater as its final control element. Before entering the drying chamber, a static mixer homogenises the temperature by mixing the gas. The sample is put in the sample holder (SH) inside the drying chamber and is supported on a weighing balance (WB) through an oil-sealed shaft. The cross-sectional area and depth of the sample holder are 45 mm × 75 mm and 5 mm, respectively. The drying chamber has a uniform cross-sectional area of 90 mm × 110 mm. The sample's weight history is recorded on a computer (C). It is possible to take a reading every 12 seconds (Mendieta *et al.*, 2015).

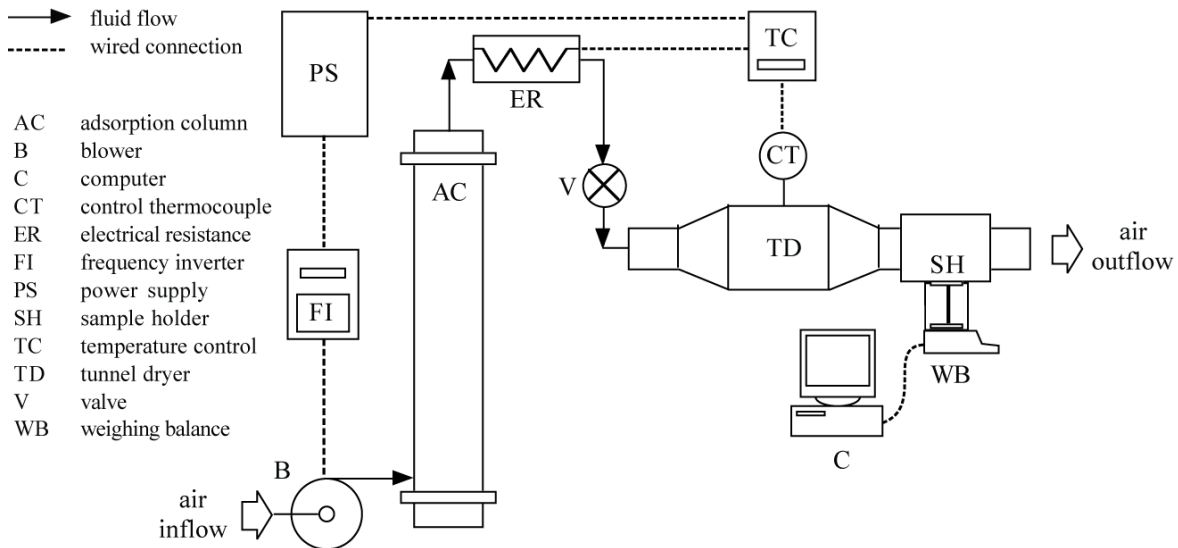


Fig. 1 A schematic diagram of a tunnel drying system.

### 2.3 Experimental procedure

The experiments were performed at several controlled conditions of temperature (50, 60, and 70 °C) and air velocity (1.0, 1.5, and 2.0 m/s). Before starting an experiment, the apparatus was run for at least half an hour to obtain steady-state conditions. The sample was loaded evenly within the sample holder, which

covered the whole drying area. The sample holder was put into the tunnel dryer. The drying time and mass of the sample were recorded. The test was stopped until the mass was invariable. After drying by the apparatus above, the sample was further dried in an oven at 110 °C for 24 hours to determine its oven-dry mass ( $m_s$ ). The initial mass, drying mass and oven-dry mass were determined with a precise analytical balance. All the drying experiments were performed in triplicate. Post-processing of these data yields drying kinetics.

## 2.4 Drying kinetics

The moisture content is computed as follows:

$$X_i = X_{i-1} + \frac{1}{m_s} \left( \frac{m_i - m_{i-1}}{t_i - t_{i-1}} \right) \quad (1)$$

where  $X$  is the moisture content at any time (dry basis),  $m$  is the mass of the sample at any time, and  $t$  is the time. The drying rate is defined as:

$$N_v = -\frac{m_s}{A_s} \frac{dX}{dt} \quad (2)$$

where  $N_v$  is the drying rate at any time and  $A_s$  is the drying area. Using the moisture content data as a function of time and a centred approximation of the derivative, it is possible to determine the drying rate as follows (Picado *et al.*, 2006):

$$N_v(X_i) = -\frac{m_s}{A_s(X_i)} \left( \frac{X_{i+1} - X_{i-1}}{t_{i+1} - t_{i-1}} \right) \quad (3)$$

The processing of the experimental data is performed using a program written in MATLAB®, this program reads the experimental data obtained and plots the drying curves and drying rate curves according to Eqs. (1) and (3).

The characteristic drying curve (CDC) concept, firstly introduced by van Meel (1958), relies on an appropriate transformation of the drying rate curve coordinates to look for a single normalised drying rate curve, which does not depend on external parameters (e.g., air conditions). The variable transformations proposed by van Meel (1958) are:

$$\phi = \frac{X_i - X_{eq}}{X_{cr} - X_{eq}} \quad (4)$$

and

$$f = \frac{N_v}{N_w} \quad (5)$$

where  $\phi$  is the characteristic moisture content,  $f$  is the relative drying rate,  $X_{eq}$  is the equilibrium moisture content,  $X_{cr}$  is the critical moisture content, and  $N_w$  is the drying rate at the constant rate period. The general form of the CDC is given by  $f = f(\phi)$ .

By plotting  $f$  vs.  $\phi$  at the different temperatures tested, a group of curves is obtained whose behaviour, if common, describes a characteristic drying curve to which a mathematical function (e.g., a polynomial function) can be determined. It is assumed that a unique relationship between  $f$  and  $\phi$  can be found for a specific material.

## 2.5 Thin-layer drying models

The moisture content of drying sample at time  $t$  can be transformed to be moisture ratio ( $MR$ ):

$$MR = \frac{X_i - X_{eq}}{X_0 - X_{eq}} \quad (6)$$

where  $X_0$  is the initial moisture content. In the literature, many models describing the diffusion mechanism and thus the evolution of the moisture loss during the drying process were reported. All these models are either empirical models based on experimental drying curves, diffusive models based on Fick's, or models based on heat and mass balance during the drying process. The empirical models are generally formulated from the direct relationship between the moisture ratio and drying time to model the thin-layer drying of foods. Recently, Buzrul (2022) analysed several empirical models and the drawbacks associated with their use. A list of suggested empirical models was reported (see Table 1).

Table 1 Suggested thin-layer drying models (Buzrul, 2022).

Model No.	Model Name	Model Equation
1	Lewis	$MR = \exp(-k \cdot t)$
2	Page	$MR = \exp(-k \cdot t^n)$
3	Modified Page I	$MR = \exp\left[-(k \cdot t)^n\right]$
4	Weibull	$MR = \exp\left[-\left(\frac{t}{k}\right)^n\right]$
5	Weibull I	$MR = 10^{-\left(\frac{t}{k}\right)^n}$
6	Modified two-term III	$MR = a \cdot \exp(-k \cdot t) + (1-a) \cdot \exp(-k \cdot a \cdot t)$

The experimental drying data are fitted to six (6) thin-layer drying models detailed in Table 1 using non-linear least squares regression analysis. Regression analysis is performed using MATLAB's Curve Fitting Toolbox. The coefficient of correlation ( $r$ ) is the primary criterion for selecting the best model to describe the drying curve and the highest  $r$  value is required. In addition to  $r$ , the root-mean-square error ( $RMSE$ ) and chi-square ( $\chi^2$ ) are used to determine the best fit. The highest  $r$  and the lowest  $\chi^2$  and  $RMSE$  values are required to evaluate the goodness of fit. These statistical values can be calculated as follows:

$$r = \frac{N \sum_{i=1}^N MR_{pred,i} MR_{exp,i} - \sum_{i=1}^N MR_{pred,i} \sum_{i=1}^N MR_{exp,i}}{\sqrt{\left(N \sum_{i=1}^N MR_{pred,i}^2 - \left(\sum_{i=1}^N MR_{pred,i}\right)^2\right) \left(N \sum_{i=1}^N MR_{exp,i}^2 - \left(\sum_{i=1}^N MR_{exp,i}\right)^2\right)}} \quad (7)$$

$$\chi^2 = \left[ \sum_{i=1}^N (MR_{exp,i} - MR_{pred,i})^2 \right] (N - w)^{-1} \quad (8)$$

$$RMSE = \left[ \frac{1}{N} \sum_{i=1}^N (MR_{exp,i} - MR_{pred,i})^2 \right]^{1/2} \quad (9)$$

where  $MR_{exp,i}$  is the  $i$ th experimental moisture ratio,  $MR_{pred,i}$  is the  $i$ th predicted moisture ratio,  $N$  is the number of observations, and  $w$  is the number of constants within the thin-layer drying model.

## 2.6 Determination of effective moisture diffusivity

Fick's second law of diffusion equation is used to fit the experimental drying data for the determination of effective moisture diffusivity.

$$\frac{\partial X}{\partial t} = D_{eff} \frac{\partial^2 X}{\partial z^2} \quad (10)$$

The solution of the Eq. (10) for slab geometry was solved by Crank (1975) and assumed uniform initial moisture distribution, negligible external resistance, constant diffusivity, and negligible shrinkage:

$$MR = \frac{8}{\pi^2} \sum_{n=1}^{\infty} \frac{1}{(2n-1)^2} \exp\left(-\frac{(2n-1)^2 \pi^2 D_{eff} t}{4H^2}\right) \quad (11)$$

where  $D_{eff}$  is the effective moisture diffusivity,  $H$  is the thickness of samples, and  $n$  is a positive integer. Only the first term of Eq. (11) can be used for long drying times (Erbay and Icier, 2009):

$$MR = \frac{8}{\pi^2} \exp\left(-\frac{\pi^2 D_{eff} t}{4H^2}\right) \quad (12)$$

The slope is determined by plotting  $\ln(MR)$  against time ( $t$ ) according to Eq. (12).

$$Slope = \frac{\pi^2 D_{eff}}{4H^2} \quad (13)$$

$D_{eff}$  varies with internal conditions, such as the temperature of the product, the moisture content, and the structure. This is harmonious with the assumption of the thin-layer concept.

## 2.7 Computation of activation energy

The dependence of the effective moisture diffusivity on the temperature is described by the Arrhenius equation:

$$D_{eff} = D_0 \exp\left(-\frac{E_a}{R(T + 273.15)}\right) \quad (14)$$

where  $D_0$  is the pre-exponential factor of Arrhenius equation,  $E_a$  is the activation energy,  $R$  is the universal gas constant, and  $T$  is the temperature.

### 3. RESULTS AND DISCUSSION

#### 3.1 Drying characteristics

The variation of moisture content with time at air temperatures of 50, 60, and 70 °C and air velocities of 1.0, 1.5, and 2.0 m/s are shown in Fig. 2. The moisture content of the samples decreased exponentially with time. As expected, an increase in air temperature reduces the time required to reach any given level of moisture content. This can be explained by increasing temperature difference between the drying the drying air and the samples and the resultant moisture migration. Similar behaviour was observed for air velocities.

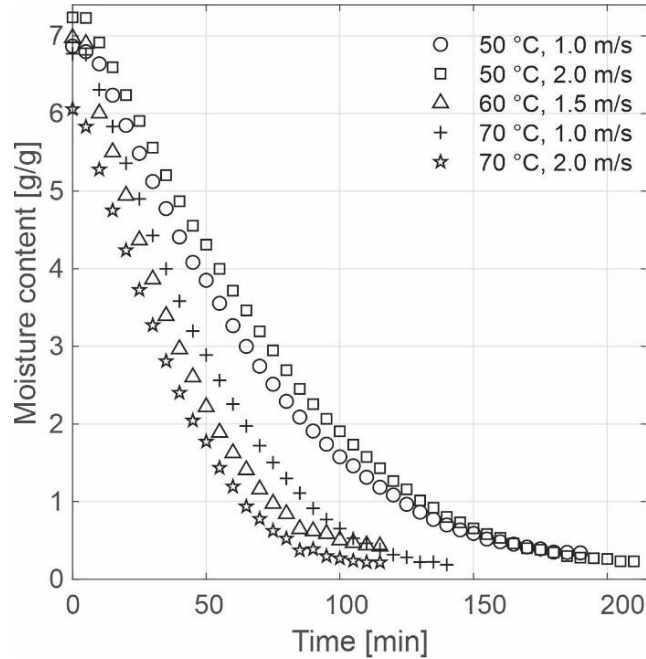


Fig. 2 Drying curves at various temperatures and air velocities.

Drying rates were estimated based on Eq. (3) and are shown in Fig. 3. An important influence of air temperature on drying rate is observed. As expected, an increase in air temperature increases the drying rate because higher air temperature causes a higher reduction of moisture content - in other words, at high temperatures the transfer of heat and mass is high and moisture loss is excessive. Similar behaviour was observed for air velocities. As can be seen from Fig. 3, no constant rate period was observed in the drying of noni; the drying process took place at a falling rate period. Shrinkage during drying was not considered in calculating the drying rates.

The drying rate and moisture content are normalised by the constant drying rate and critical moisture content, respectively. However, for noni no constant drying rate period was observed and another approach must be found to normalise the drying data. In this case, the critical moisture content and the maximum drying rate were determined at the beginning of the falling rate period (Bellagha *et al.*, 2002; Picado *et al.*, 2006).

In Fig. 4, experimental drying data are plotted to represent  $f = f(\phi)$ . Figure 4 shows that all drying curves obtained with the characteristic moisture content ( $\phi$ ) and relative drying rate ( $f$ ), for the different tested

conditions, fall into a tight band, thus indicating that the effect of variation in different conditions is small over the range tested.

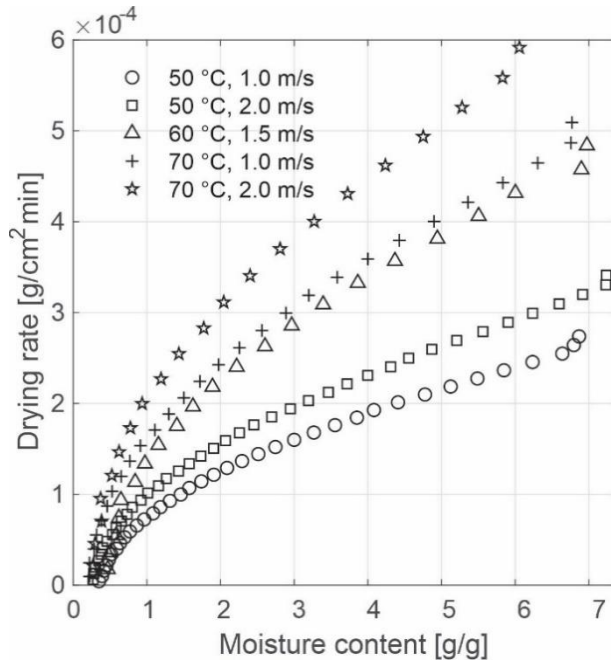


Fig. 3 Drying rate curves at various temperatures and air velocities.

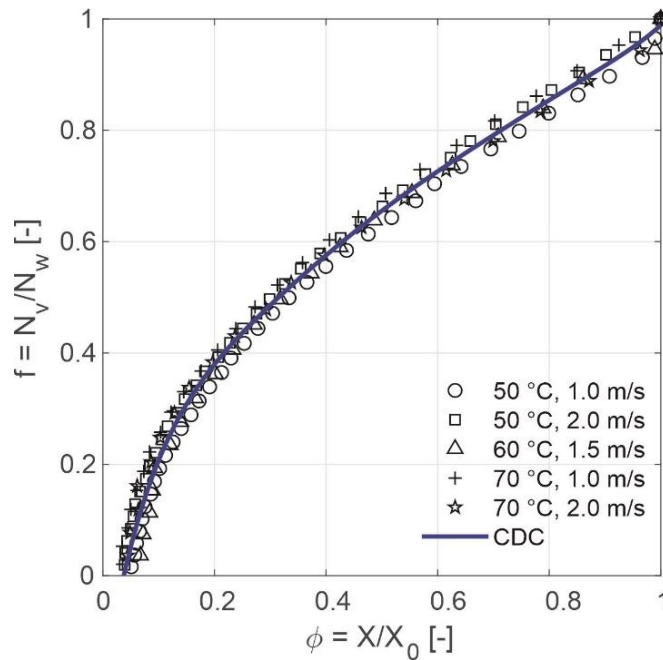


Fig. 4 Characteristic drying curve for noni.

The regression analysis was performed using MATLAB®'s Curve Fitting Tool to find the best equation for the noni characteristics drying curve. A polynomial equation was found to fit the best the experimental data:

$$f = 6.11\phi^5 - 20.02\phi^4 + 24.57\phi^3 - 15.65\phi^2 + 5.99\phi - 0.17 \quad (15)$$

### 3.2 Fitting of drying curves

The drying data obtained from the experiments were fitted by six (6) thin-layer drying models reported in Table 1. The results of statistical analysis on the thin-layer drying models are given in Tables 2-4. The best model describing the thin-layer drying characteristics of noni was chosen as the one with the highest  $r$  and the lowest  $RMSE$  and  $\chi^2$ .

The results showed that the Page model exhibited the best fit to drying experimental data. The Page model exhibits a better suitability with the experimental data not only because of the lower number of coefficients, but also due to the form of the model equation (Picado *et al.*, 2017; Buzrul, 2022). As known, the Page model is widely used as the basis for most semi-theoretical thin-layer models (Erbay and Icier, 2009). Additionally, the Page model has been adopted as a standard by ASABE in thin-layer modelling of agricultural and biological product (ASABE, 2014).

Table 2 Results of statistical analysis for  $T = 50$  °C and 1.0 m/s.

Model	Coefficients	$r$	$RMSE$	$\chi^2$
Lewis	$k = 0.01362$	0.9874	0.0490	2.4013 E-3
Page	$k = 0.003191, n = 1.33$	0.9996	0.0089	7.8514 E-5
Modified Page I	$k = 0.01327, n = 1.33$	0.9996	0.0089	7.8514 E-5
Weibull	$k = 75.34, n = 1.33$	0.9996	0.0089	7.8514 E-5
Weibull I	$k = 141.1, n = 1.33$	0.9996	0.0089	7.8514 E-5
Modified two-term III	$k = 75.43, a = 0.0001806$	0.9506	0.0497	2.4708 E-3

Table 3 Results of statistical analysis for  $T = 60$  °C and 1.5 m/s.

Model	Coefficients	$r$	$RMSE$	$\chi^2$
Lewis	$k = 0.02262$	0.9896	0.0450	2.0265 E-3
Page	$k = 0.007282, n = 1.291$	0.9991	0.0134	1.7827 E-4
Modified Page I	$k = 0.02208, n = 1.291$	0.9991	0.0134	1.7827 E-4
Weibull	$k = 45.29, n = 1.291$	0.9991	0.0134	1.7827 E-4
Weibull I	$k = 86.43, n = 1.291$	0.9991	0.0134	1.7827 E-4
Modified two-term III	$k = 76.3, a = 0.0002963$	0.9895	0.0461	2.1254 E-3

In this study, the validation of the Page model has also been confirmed by comparing the predicted moisture ratios to the experimental values at a temperature of 50 °C and at an air velocity of 1.0 m/s (see Fig. 5). The predicted data is banded around the straight line that showed the suitability of the Page model in describing the drying characteristics of the thin-layer noni. Similar results have been reported for other food materials (Picado *et al.*, 2017; Mendieta *et al.*, 2015).

Table 4 Results of statistical analysis for  $T = 70\text{ }^{\circ}\text{C}$  and  $1.0\text{ m/s}$ .

Model	Coefficients	$r$	RMSE	$\chi^2$
Lewis	$k = 0.01859$	0.9821	0.0613	3.7607 E-3
Page	$k = 0.003175, n = 1.431$	0.9997	0.0076	5.7370 E-5
Modified Page I	$k = 0.01796, n = 1.431$	0.9997	0.0076	5.7370 E-5
Weibull	$k = 55.68, n = 1.431$	0.9997	0.0076	5.7370 E-5
Weibull I	$k = 99.73, n = 1.431$	0.9997	0.0076	5.7370 E-5
Modified two-term III	$k = 77.58, a = 0.0002395$	0.9820	0.0625	3.9074 E-3

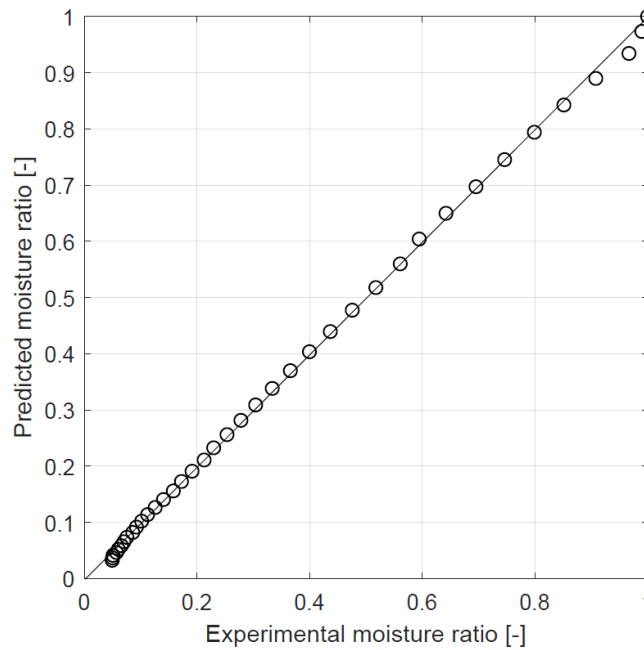


Fig. 5 Comparison of the experimental and predicted moisture ratios at a temperature of  $50\text{ }^{\circ}\text{C}$  and at an air velocity of  $1.0\text{ m/s}$ .

### 3.3 Effective moisture diffusivity

The values of effective moisture diffusivity were calculated using Eq. (14). The  $D_{eff}$  values were varied in the range of  $1.77 \times 10^{-7}$  to  $3.33 \times 10^{-7}\text{ m}^2/\text{s}$  from  $50$  to  $70\text{ }^{\circ}\text{C}$  and from  $1.0$  to  $2.0\text{ m/s}$ . It was observed that  $D_{eff}$  values increased with increasing drying temperature. When samples were dried at higher temperature, increased heating energy would increase the activity of water molecules leading to higher moisture diffusivity (Xiao *et al.*, 2010).

### 3.4 Activation energy

A plot of  $\ln(D_{eff})$  against  $1/(T + 273.15)$  gave a straight line ( $r = 0.9763$ ), which is shown in Fig. 6. The slope ( $-E_a/R$ ) of the straight line was obtained and by using the Arrhenius relationship, the activation

energy was obtained to be 3.34 kJ/mol. Similar values have been reported for other food materials (Erbay and Icier, 2009).

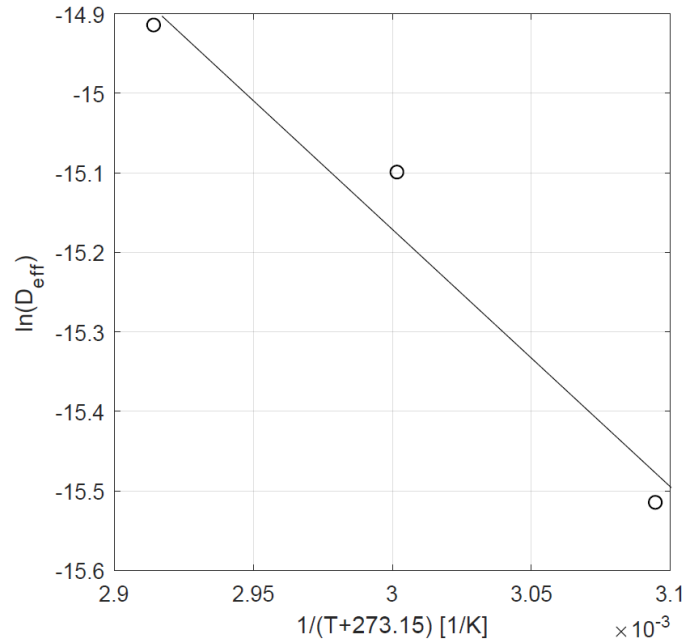


Fig. 6 The relationship of  $\ln(D_{eff})$  and  $1/(T + 273.15)$  at various air velocities.

Semi-theoretical and empirical models, such as Page model, provide adequate representation of experimental results although the parameters of these models have not physical meaning. Semi-theoretical and empirical models do not need assumptions of material properties that from practical point of view is very important. Therefore, these models give usually good results for engineering application. Semi-theoretical and empirical models, however, frequently did not enable the simulation of experiments performed under different conditions to those used to identify the model parameters.

#### 4. CONCLUSIONS

The drying kinetics of noni (*Morinda citrifolia* L.) was experimentally investigated in a laboratory tunnel dryer at air temperatures of 50, 60, and 70 °C and air velocities of 1.0, 1.5, and 2.0 m/s. Noni did not show a constant drying rate period under the experimental conditions employed and showed only a falling drying rate period, such as most food products. The moisture content of noni decreased continually with drying time. As expected, an increase in the air temperature or air velocity reduces the time required to reach any given level of moisture content. Further, a non-linear regression procedure was used to determine the characteristic drying curve. The experimental drying data of noni were employed to fit thin-layer models. Under the evaluated experimental conditions, the Page model provided the best representation of thin-layer drying characteristics of noni. The effective moisture diffusivity ranged from  $1.77 \times 10^{-7}$  to  $3.33 \times 10^{-7}$  m<sup>2</sup>/s. The activation energy required to move the water out from noni during the drying process was found to be 3.34 kJ/mol.

#### ACKNOWLEDGEMENTS

The authors gratefully acknowledge the financial support provided by the Swedish International Development Cooperation Agency (Sida).

## CONFLICT OF INTEREST

The authors declare that there is no conflict of interest regarding the publication of this article.

## NOTATION

$a$	Constant	(-)
$A_s$	Drying area	(m <sup>2</sup> )
$D$	Diffusivity coefficient	(m <sup>2</sup> s <sup>-1</sup> )
$E_a$	Activation energy	(J mol <sup>-1</sup> )
$f$	Relative drying rate	(-)
$H$	Thickness	(m)
$k$	Constant	(-)
$m$	Mass	(kg)
$MR$	Moisture ratio	(-)
$n$	Constant	(-)
$N$	Number of observations	(-)
$N_v$	Drying rate	(kg m <sup>-2</sup> s <sup>-1</sup> )
$N_w$	Drying rate at the constant rate period	(kg m <sup>-2</sup> s <sup>-1</sup> )
$r$	Coefficient of correlation	(-)
$R$	Universal gas constant	(J mol <sup>-1</sup> K <sup>-1</sup> )
$RMSE$	Root-mean-square error	(-)
$t$	Time	(s)
$T$	Temperature	(K)
$w$	Number of constants	(-)
$X$	Moisture content, dry basis	(kg kg <sup>-1</sup> )
$z$	Distance	(m)

### Greek Letters

$\phi$	Characteristic moisture content	(-)
$\chi^2$	Chi-square	(-)

### Subscripts

$i$	$i$ th value	$eq$	Equilibrium value
$cr$	Critical value	$s$	Solid
$eff$	Effective value	$0$	Initial

## REFERENCES

Alonso, J., & Guerrero-Santos, R. (2016). Anthraquinones from *Morinda citrifolia* root extracts as styrene free-radical bulk polymerization inhibitors. In *Proceedings of the 28th Inter-American Congress of Chemical Engineering (IACChE 2016)*. Paper No. 366. Cusco, Peru.

ASABE (2014). Thin-layer drying of agricultural crops. ASAE ANSI/ASAE S448.2. American Society of Agricultural and Biological Engineers, USA. URL: <https://elibrary.asabe.org/abstract.asp?aid=45096&t=2>

Bellagha, S., Amami, E., Farhat, A., & Kechaou, N. (2002). Drying kinetics and characteristic drying curve of lightly salted sardine (*Sardinella aurita*). *Drying Technology*, 20(7), 1527-1538. doi: [10.1081/DRT-120005866](https://doi.org/10.1081/DRT-120005866)

Buzrul, S. (2022). Reassessment of thin-Layer drying models for foods: A critical short communication. *Processes*, 10(1), 118. doi: [10.3390/pr10010118](https://doi.org/10.3390/pr10010118)

Chan-Blanco, Y., Vaillant, F., Perez, A.M., Reynes, M., Brillouet, J.M., & Brat, P. (2006). The noni fruit (*Morinda citrifolia* L.): A review of agricultural research, nutritional and therapeutic properties. *Journal of Food Composition and Analysis*, 19(6-7), 645-654. doi: [10.1016/j.jfca.2005.10.001](https://doi.org/10.1016/j.jfca.2005.10.001)

Crank, J. (1975). *The Mathematics of Diffusion*, 2<sup>nd</sup> Ed. Oxford University Press.

Erbay, Z., & Icier, F. (2009). A review of thin layer drying of foods: theory, modeling, and experimental results. *Critical Reviews in Food Science and Nutrition*, 50(5), 441-464. doi: [10.1080/10408390802437063](https://doi.org/10.1080/10408390802437063)

Lin, C-H., Huang, T-C., Chen, H-H., & Sheu, S-C. (2020). Ester formation in intermittently dried noni fruit (*Morinda citrifolia* L.). *Drying Technology*, 38(9), 1186-1193. doi: [10.1080/07373937.2019.1624973](https://doi.org/10.1080/07373937.2019.1624973)

Mendieta, R., Haerinejad, M., & Picado, A. (2015). Determination of suitable thin-layer drying models for brewer's yeast (*Saccharomyces cerevisiae*). *Nexo*, 28(2), 58-66. doi: [10.5377/nexo.v28i2.3421](https://doi.org/10.5377/nexo.v28i2.3421)

Mireles-Arriaga, A.I., Ruiz-López, I.I., Hernández-García, P.A., Espinosa-Ayala, E., López-Martínez, L. X., & Márquez-Molina, O. (2016). The impact of convective drying on the color, phenolic content, and antioxidant capacity of noni (*Morinda citrifolia* L.). *Food Science and Technology*, 36(4), 583-590. doi: [10.1590/1678-457X.00415](https://doi.org/10.1590/1678-457X.00415)

Nelson, S.C. (2003). *Morinda citrifolia* L. University of Hawai'i at Manoa, College of Tropical Agriculture and Human Resources (CTAHR), Department of Plant & Environmental Protection Sciences (PEPS). Hawaii, USA. URL: [https://www.ctahr.hawaii.edu/noni/downloads/morinda\\_species\\_profile.pdf](https://www.ctahr.hawaii.edu/noni/downloads/morinda_species_profile.pdf)

Picado, A., Mendieta, R., & Martínez, J. (2006). Cinética de secado de la levadura cervecera (*Saccharomyces cerevisiae*). *Nexo*, 19(1), 49-56. doi: [10.5281/zenodo.3576375](https://doi.org/10.5281/zenodo.3576375)

Picado, A., Solís, R., & Gamero, R. (2017). Thin-layer drying characteristics and modelling of instant coffee solution. In *Proceedings of the 19th International Conference on Chemical Engineering (ICCE 2017)*. Paper No. 17US120037. Miami, USA. doi: [10.5281/zenodo.4515793](https://doi.org/10.5281/zenodo.4515793)

Quequeto, W.D., Resende, O., Silva, P.C., Silva, F.A.S., & Silva, L.D.M. (2019). Drying kinetics of noni seeds. *Journal of Agricultural Science*, 11(5), 250-258. doi: [10.5539/jas.v11n5p250](https://doi.org/10.5539/jas.v11n5p250)

van Meel, D.A. (1958). Adiabatic convection batch drying with recirculation of air. *Chemical Engineering Science*, 9(1), 36-44. doi: [10.1016/0009-2509\(58\)87005-0](https://doi.org/10.1016/0009-2509(58)87005-0)

Wang, R., Wang, L., Zhang, L., Wan, S., Li, C., & Liu, S. (2022). Solvents effect on phenolics, iridoids, antioxidant activity, antibacterial activity, and pancreatic lipase inhibition activity of noni (*Morinda citrifolia* L.) fruit extract. *Food Chemistry*, 377, 131989. doi: [10.1016/j.foodchem.2021.131989](https://doi.org/10.1016/j.foodchem.2021.131989)

Xiao, H.W., Pang, C.L., Wang, L.H., Bai, J.W., Yang, W.X., & Gao, Z.J. (2010). Drying kinetics and quality of Monukka seedless grapes dried in an air-impingement jet dryer. *Biosystems Engineering*, 105(2), 233-240. doi: [10.1016/j.biosystemseng.2009.11.001](https://doi.org/10.1016/j.biosystemseng.2009.11.001)

Zhang, C., Fu, N., Quek, S.Y., Zhang, J., & Chen, X.D. (2019). Exploring the drying behaviors of microencapsulated noni juice using reaction engineering approach (REA) mathematical modelling. *Journal of Food Engineering*, 248, 53-61. doi: [10.1016/j.jfoodeng.2018.12.016](https://doi.org/10.1016/j.jfoodeng.2018.12.016)